Combustion and Flame 224 (2021) 66–72

Contents lists available at ScienceDirect

Combustion and Flame

journal homepage: www.elsevier.com/locate/combustflame

Impact of vitiation on flow reactor studies of jet fuel combustion chemistry

Kun Wang[1], Rui Xu, Craig T. Bowman*, Hai Wang

Mechanical Engineering Department, Stanford University, Stanford, CA 94305 USA

ARTICLE INFO

Article history:
Received 27 August 2020
Revised 24 October 2020
Accepted 25 October 2020
Available online 4 November 2020

Keywords:
Flow reactors
Jet fuels
Vitiated reactions
Pyrolysis
Oxidation
Hybrid chemistry models

ABSTRACT

Flow reactors are commonly employed in investigations of the pyrolysis and oxidation chemistry of fuels. Typical flow reactors use either electrical heaters or vitiation heaters to provide the energy to preheat the reactants to the desired experimental conditions. The present study seeks to determine the impact of vitiation on flow reactor studies of fuel combustion chemistry by conducting both fuel pyrolysis and oxidation experiments in a flow reactor in which either an electrical heater or a vitiation heater is used as the energy source. Other than the heater all other aspects of the flow reactor are identical. Two fuels relevant to air-breathing propulsion systems were investigated – Jet A and JP-10. Profiles of the stable reaction products were measured using gas chromatography for a temperature of 1030 K at a pressure of 1 atmosphere, with residence times between 30 ms and 70 ms. The primary hydrocarbon products for Jet A pyrolysis and oxidation were C_2H_4, C_3H_6, CH_4, C_4H_8, C_6H_6 and C_7H_8. For JP-10, in addition to these species, cyclopentene (C_5H_8) and cyclopentadiene (C_5H_6) were measured. Under the conditions investigated, vitiation decreases the reaction times scales for both pyrolysis and oxidation. However, the product yields at a fixed fuel conversion were nearly identical for both the vitiated and non-vitiated experiments. Current kinetic models for Jet A and JP-10 pyrolysis and oxidation adequately captured the observed effects of vitiation on the stable species profiles.

1. Introduction

Flow reactors are an important tool for the development and validation of reaction kinetic models for pyrolysis and oxidation of hydrocarbon fuels and fuel constituents [1–5] as well as for studies of supersonic combustion [6]. Typically, these flow reactors use either electrical heaters or vitiation heaters to preheat the reactants to the desired experimental conditions. Unlike electrical heaters, with vitiation heaters the carrier gas contains the products of combustion in addition to the fuel and oxidizer being investigated. In using vitiation heaters, the question arises as to what the impact of the additional species is on the reaction under investigation. Electrical heaters usually use nitrogen or air as the carrier gas into which a fuel is injected and rapidly mixed. The reaction progress is followed downstream in the reactor by sample extraction and species measurements are made using online analyzers such as gas chromatographs. These types of experiments provide a relatively clean background for fundamental reaction kinetics experiments. Vitiation heaters utilize pre-combustion of a fuel–oxidizer mixture so that the background gas into which the test fuel is injected comprises combustion products from the preburner. While this situation is more complex kinetically, it does resemble the combustion environment found in many practical devices where vitiation is inherent or deliberately created. Examples include high-Karlovitz-number premixed turbulent combustion in which local exhaust gas recirculation (EGR) can become significant [7], EGR in diesel engines [8] and flameless oxidation in process heaters and furnaces for NO_x reduction [9]. It is desirable to be able to reconcile data obtained from flow facilities that use both types of preheaters, and to quantify the mechanistic and kinetic differences between the resulting carrier gases.

The above question is particularly relevant to the development of Hybrid Chemistry (HyChem) models for the combustion of real, multicomponent fuels [10]. The HyChem approach assumes that high-temperature combustion of large hydrocarbon compounds proceeds from oxidative fuel pyrolysis first, followed by the oxidation of a handful of pyrolysis products, including hydrogen, methane, ethylene, propene, butene isomers, benzene and toluene to form the final combustion products. The approach relies on time histories of the pyrolysis products, measured in shock tubes and flow reactors, to formulate the lumped fuel oxidative pyrolysis

* Corresponding author.
E-mail address: ctbowman@stanford.edu (C.T. Bowman).
[1] Current address: State Key Laboratory of Engines, Mechanical Engineering Department, Tianjin University, Tianjin 300350 China.

https://doi.org/10.1016/j.combustflame.2020.10.044
0010-2180/

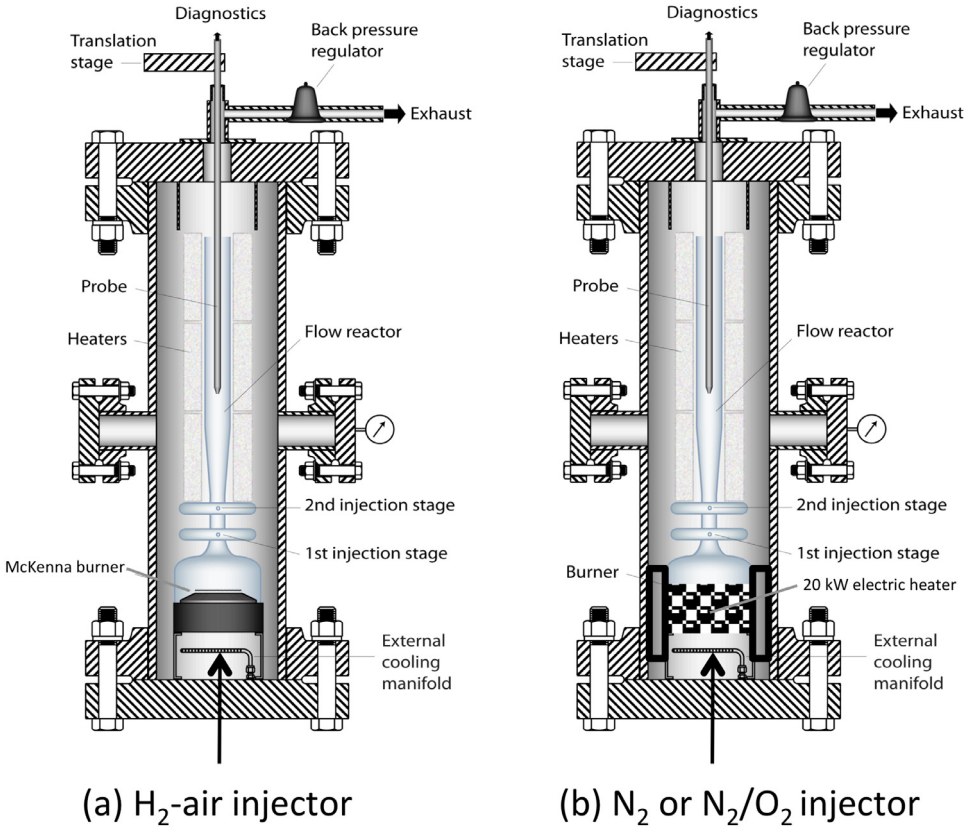

Fig. 1. The Stanford flow reactor facility.

reactions and to derive the model parameters. In previous studies [10–13], the time histories of selected species from the Stanford flow reactor were used as the basis for defining some of the key model parameters, including the ratios of C_3 and C_4 alkenes to ethylene, and the ratio of benzene to the sum of benzene and toluene. A question that arises from this approach is, how do the vitiated diluent gases impact the HyChem parameter determination? A further related question is, is the HyChem model accuracy impacted by the use of a vitiated diluent, especially considering that the ethylene and methane time histories, a set of critical data for HyChem model development, were taken from Stanford shock tubes in which either nitrogen or argon was used as the diluent. The present study seeks to address these questions by conducting both fuel pyrolysis and oxidation experiments in a flow reactor in which either an electrical heater or a vitiation heater is used as the energy source. Results are presented to show the impact of vitiated gases on the combustion chemistry of two representative fuels used in HyChem model development: a conventional Jet A and JP-10. While Jet A is a multicomponent distillate fuel, JP-10 is a synthetic, practically single-component fuel with > 96 wt% exo-tetrahydrodicyclopentadiene. The difference in the reaction behaviors of these two fuels represent, to an extent, the range of composition of different real liquid jet fuels.

2. Experimental methodology

The Stanford flow reactor facility that has been used in previous studies [5,11–15] is shown in Fig. 1a. Relevant to the current study, it is important to point out that a H_2–air vitiation heater is used to provide the energy to preheat the reactants. In the present study, the reactor was modified by replacing the McKenna burner by a 20 kW electric resistance heater, shown in Fig. 1b. The H_2–air flow to the McKenna burner in Fig. 1a is replaced by N_2 (for the pyrolysis experiments) or a N_2–O_2 mixture (for the oxidation experiments as shown in Fig. 1b for the electrical resistance heating method). All other features of the flow reactor and the sampling and measurement techniques remain unchanged. In the vitiation experiments, the composition of the McKenna burner products was predominately N_2 (~80 mol%) and water vapor (~18 mol%); trace amounts of CO_2 and Ar are also present due to the use of air for the McKenna burner. In the vitiated oxidation experiments, there was also 0.5–0.6 mol% O_2; in the vitiated pyrolysis experiments, there was 1.3 mol% H_2 and immeasurable (< 5 ppm) O_2. Additional composition information can be found in Table S1 of the Supplementary Material.

As discussed in previous publications [5,11–15], we measured the temperature and species concentration along the reactor axis using a Pt/13%Rh-Pt thermocouple coated with a passivating SiO_2 film and a propylene glycol cooled species probe with a choked inlet, both of which are attached to a computer-controlled translation stage. The quartz reactor tube is electrically heated by temperature-controlled heaters to ensure constant temperature. In the non-vitiated experiments, the power of the electric heater was adjusted until the reactor temperature reaches a prescribed value. In vitiated experiments, a H_2/air flame on a water-cooled McKenna burner provides a hot vitiated flow into the reactor. Under the vitiation condition, radicals are not present in significant quantities (< 1 ppmv based on equilibrium calculations) in the vitiated gas [5,16]. Also, a 10 ppmv of H atom addition at the reactor inlet showed no difference in the computed species profiles [16]. For all of the experiments reported here, the reactor temperature is held at 1030±4 K, where the uncertainty value includes the uncertainty due to radiation correction and temperature variations along the rector length.

Two fuels relevant to air-breathing propulsion systems were investigated – Jet A and JP-10. Both fuels and their chemical

analyses were provided by Dr. Tim Edwards from the Air Force Research Laboratory (AFRL). The Jet A, designated as the A2 fuel in the National Jet Fuel Combustion Program [17], is a petroleum-derived distillate fuel comprising many hundreds of hydrocarbon species with a composition represented by $C_{11.4}H_{21.7}$. As discussed earlier, JP-10 is exo-tetrahydrocyclopentadiene ($C_{10}H_{16}$). The liquid fuels used in the present study were fine sprayed through a glass nebulizer and injected into an in-house designed vaporizer by a precision syringe pump (Harvard Apparatus PhD, accuracy ±0.35%) before being introduced into the reactor with a heated nitrogen carrier gas. In the present experiments, the fuel loadings at the reactor inlet were 300 ppmv to 400 ppmv.

The extracted gas samples are sent to a 4-column micro gas chromatograph with thermal conductivity detectors (INFINICON 3000) or to a paramagnetic analyzer (PMA) or a non-dispersive infrared analyzer (NDIR) that provide on-line real-time detection of the concentrations of the stable compounds. Both wet and dry sampling was employed. Wet sampling was used for measuring fuel components and aromatics. Dry sampling was used for all other species. In wet sampling, the extracted gas samples are directly transferred by a diaphragm pump to the GC through stainless steel tubing that is maintained at 130°C. In dry sampling, the extracted gas samples pass through a refrigerated cold trap at 5 °C which reduces the water content to less than 2 mol% and then through a Drierite desiccant bed to remove the remaining water. The dry sample then passes through the diaphragm pump and is split into three different streams. The first stream goes to the on-line GC while the second and third streams go to the PMA for O_2 measurement or the NDIR for CO and CO_2 measurement for comparison with the GC data. Calibration of the GC was done using multicomponent calibration mixtures provided by Praxair. The quoted compositional uncertainty associated with these mixtures is nominally ±2%. The total uncertainty in measured species mole fractions is ±2% to ±5%.

3. Kinetic modeling

The flow reactor data obtained in the present study were modeled using previously reported HyChem models for Jet A [11] and JP-10 [12]. These models may be downloaded from https://web.stanford.edu/group/haiwanglab/HyChem/pages/download.html. The compositions of the initial mixtures are provided in the Supplementary Materials. To account for the fuel-oxidizer mixing at the entrance of the flow reactor, a one-dimensional mixing-reaction model developed by Zwietering [18] was employed. In the present study, the mixing-reaction model was incorporated into the PFR module of CHEMKIN-PRO using two inlet streams (carrier gas + injected fuel-N_2) in conjunction with the kinetic models to simulate the species profiles as functions of time. Details of the implementation of this modeling approach in the flow reactor are described in [14]. Typical mixing times are small (2–3 ms) compared to the total residence times in the reactor (30–70 ms). As will be shown later, the mixing times are much shorter than the initial fuel pyrolysis time in the non-vitiated experiment, but they overlap, to an extent, with the fuel pyrolysis time in the vitiated experiments. In the simulations, the measured temperature profiles were utilized. Due to the low fuel loadings in the experiments (< 400 ppmv) and the electric heaters along the reaction tube, the axial temperature variation outside of the mixing region is small (< 5 K).

4. Results

Five different experiments were conducted in the present study. As summarized in Table 1, three experiments used Jet A as the fuel, in which the diluent gas was either from a vitiated source

Table 1
Summary of conditions of key experiments, all at 1030 K temperature and 1 atm pressure.

Expt.	Fuel	Condition	Equivalence ratio, ϕ	Fuel conc. (ppmv)
1	Jet A	non-vitiated	∞[a]	316 ± 5
2	Jet A	non-vitiated	1.0	316 ± 5
3	Jet A	vitiated	1.0	314 ± 5
4	JP-10	non-vitiated	0.94	408 ± 5
5	JP-10	vitiated	0.95	358 ± 6

[a] Pyrolysis in N_2.

at unity equivalence ratio, or a non-vitiated (by electric heating) O_2–N_2 mixture (without H_2 addition) also at unity equivalence ratio, or a non-vitiated N_2 flow, all at the same reactor temperature of 1030 K and 1 atm pressure. For JP-10, vitiated and non-vitiated comparisons were made at 0.94 and 0.95 equivalence ratios, respectively, due to slight difference in the fuel loading. The accuracy of the fuel concentrations (~ ±1.5%) is estimated from the accuracies of the syringe pump, and the uncertainties in the fuel composition and gas metering. As in our earlier studies [5,10–13, 16], the carbon balance is typically at or greater than 90%.

Figure 2 shows a comparison of the species profiles for pyrolysis (Experiment 1) and oxidation (Experiment 2) of Jet A for the non-vitiated experiments in which N_2 was the sole diluent. It can be seen that the mixing model captures the measured, initial oxygen concentration profile (Experiment 2 only) well. While the experimental data suggest that the mixing time is 1–2 ms, the mixing model shows it to be 2–3 ms. In either case, the fuel pyrolysis time is longer, as evidenced by the measured fuel concentration in the first few milliseconds being in close agreement with the initial fuel concentrations listed in Table 1, and no appreciable products formed in the first 5 msec. For the conditions of the experiments, the species profiles are nearly identical for both pyrolysis and oxidation, and the O_2 that is present in the oxidation experiment remains unchanged after the mixing region. The carbon present in the measured product species accounts for over 90% of the total carbon converted from Jet A. No CO_2 was detected in the oxidation experiment, although some CO was detected at a later reaction time (e.g. in Experiment 3, vitiated oxidation of Jet A, 59 ppm CO was detected at 28 ms or < 5% of the total carbon mass among the reaction products was measured). As a key assumption of the HyChem modeling approach [10,11], the presence of oxygen has only a minimal effect on the fuel breakdown process in terms of the distribution of the key pyrolysis products and their production rates. The insensitivity to oxygen and the decoupling of the earlier, rapid fuel pyrolysis from the later, slow oxidation of the pyrolysis products is quite universal. The phenomenon was observed for a range of hydrocarbon fuels in a variety of shock-tube experiments [19–21] (and again, demonstrated here). Oxygen has, at the best, a small effect of speeding up the fuel pyrolysis because of a somewhat increased rate of H-abstraction of the fuel molecules by O_2, HO_2 and to a small extent, OH that is produced during the oxidative pyrolysis process.

Also shown in Fig. 2 are the results from the HyChem simulations using the Jet A model reported in [11]. Overall, the model reproduces the species time profiles well; it distinguishes the small difference due to oxygen presence, except that the effect predicted by the model is somewhat larger than the experimental data. The HyChem model does not consider pyrolysis products larger than the C_4 alkenes and aromatics larger than toluene, hence it effectively lumps all species not accounted for into the fuel. For this reason, the calculated Jet A concentrations are slightly higher than the experimentally measured concentrations especially during the early stage of the reaction. The initial high fuel mole fraction and the rapid decrease in calculated fuel mole fraction at very short

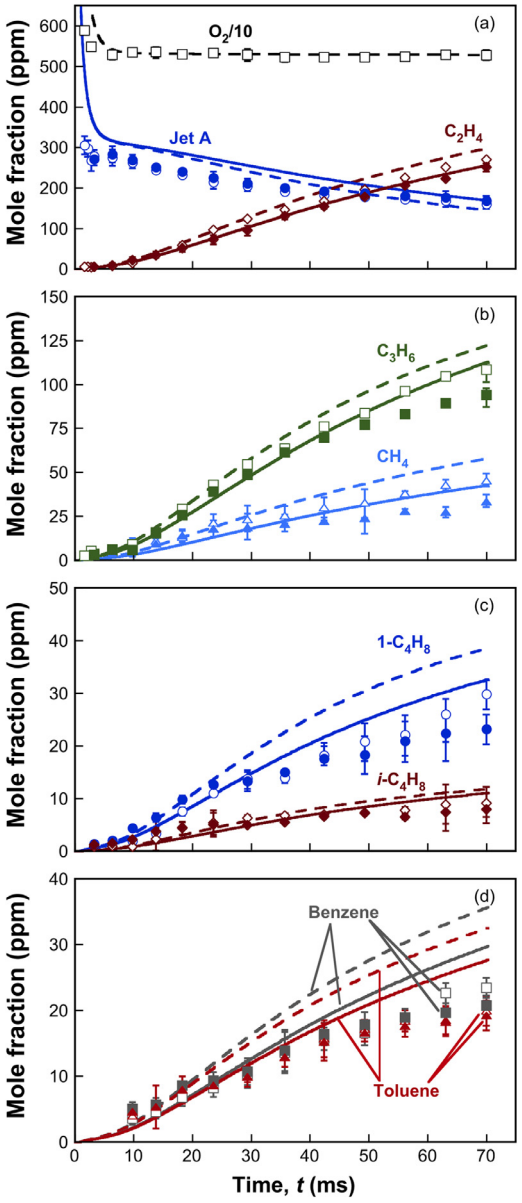

Fig. 2. Experimental (symbols) and computed (lines) species profiles in non-vitiated pyrolysis and oxidation of Jet A at 1030 K and 1 atm. Experiment 1 (pyrolysis): filled symbols and solid lines; Experiment 2 (oxidation): open symbols and dashed lines. See Table 1 for experimental conditions. The vertical bars represent scatter in the experimental data from multiple experiments. The computed initial fuel and oxygen mole fraction values are higher than the nominal values given in Table 1 because of the mixing model used in the simulations.

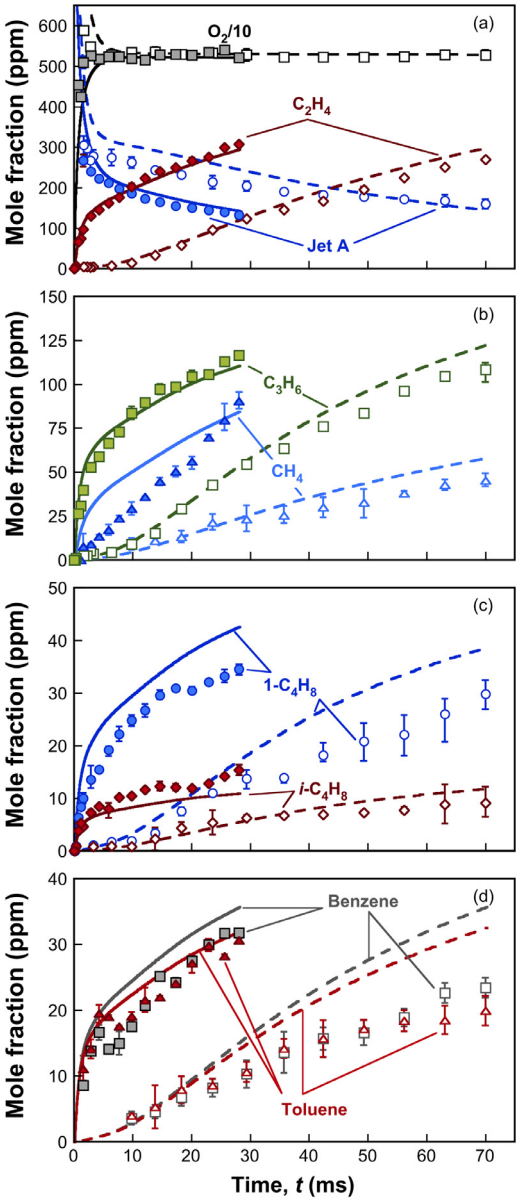

Fig. 3. Experimental (symbols) and computed (lines) species profiles in vitiated and non-vitiated oxidation of Jet A at 1030 K and 1 atm with $\phi = 1.0$. Experiment 3 (vitiated oxidation): filled symbols and solid lines; Experiment 2 (non-vitiated oxidation): open symbols and dashed lines. See Table 1 for experimental conditions. The vertical bars represent scatter in the experimental data from multiple experiments. The computed initial fuel and oxygen mole fraction values are higher than the nominal values given in Table 1 because of the mixing model used in the simulations.

residence times is due to mixing of the injected fuel with the product gases of the vitiation heater.

Figure 3 shows a comparison of the species profiles for Jet A oxidation for a non-vitiated experiment (Experiment 2) with a vitiated experiment for nearly identical conditions (Experiment 3). The most striking observation in Fig. 3 is that vitiation produces a significant reduction in reaction time for a similar fuel conversion. The HyChem model captures the effect of lack of vitiation well, keeping in mind that its development was based on the vitiated experiments, rather than the non-vitiated experiments. The model overpredicts the formation rates of several of the larger pyrolysis species to an extent, especially benzene and toluene under the non-vitiated condition. The cause for the discrepancy clearly requires further study, although the observed discrepancy is unlikely to cause any appreciable problem for the HyChem model to predict basic combustion properties (e.g., ignition delay and flame speed), because the concentrations of these larger species are small. A recent study [22] shows that the predictive capability of the HyChem model is the most sensitive to the ethylene yield, and is insensitive to benzene and toluene yields.

The most important experimental observations of Experiments 1–3 are summarized in Fig. 4, which shows the experimentally determined carbon distribution for Jet A at a fixed fuel conversion (47%) for both vitiated and non-vitiated conditions. Except for methane, the yields of all other species are similar; their values are typically within the respective measurement uncertainties at this value of fuel conversion. Such a similarity in fact extends over a fairly wide range of fuel conversion over the respective time

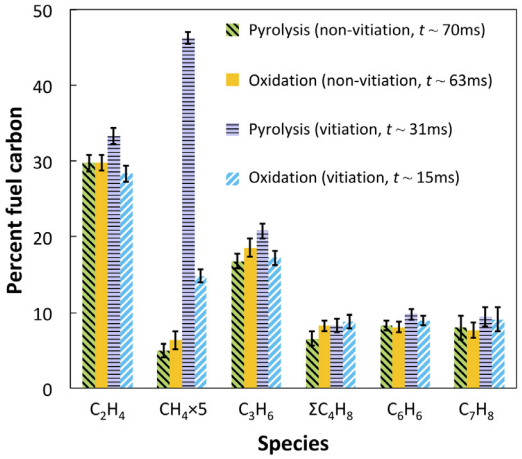

Fig. 4. Experimentally-observed carbon distributions for Jet A at 47% fuel conversion under vitiated (oxidation) and non-vitiated conditions at 1030 K. The vertical bars represent scatter in the experimental data from multiple experiments. The carbon distribution under vitiated pyrolysis experiment was obtained at 1010 K and 37% Jet A conversion (maximum for the experiment). The conditions of the vitiated pyrolysis experiment at 1010 K (not shown in Table 1) are provided in Table S1 of the Supplementary Materials.

windows of the observation. The methane yield in the vitiated oxidation experiment is about a factor of three of the yield in the non-vitiated experiment. Also included in Fig. 4 are the data acquired for vitiated pyrolysis of Jet A under a comparable condition (Experiment 6 in Table S1 of the Supplementary Materials). As expected and with the exception of methane (which is about a factor of nine times the methane yield in the non-vitiated pyrolysis experiment), the product distribution is largely the same as those of the other experiments.

Reaction path analysis indicates that the larger methane production in the vitiated experiments is caused by the presence of a large amount of H_2O and its reaction with the methyl radical that leads to methane production via:

$$CH_3+H_2O \rightarrow CH_4+OH$$

This reaction is inactive in the non-vitiated environment, in which methane is produced from the reactions

$$CH_3+H(+M) \rightarrow CH_4(+M)$$

and

$$C_3H_6+CH_3 \rightarrow a-C_3H_5+CH_4.$$

The methyl radical (CH_3) is one of the key products of the β-scission of the fuel radicals under both the vitiated and non-vitiated conditions. In the vitiated experiments, the conversion of water to the OH radical speeds up the overall reaction process, leading to increased overall reaction rates of fuel breakdown and pyrolysis products generation, as it can be seen in Fig. 3. In contrast, under the non-vitiated condition, the destruction of the H atom from its combination with the methyl radical leads to a slowdown in fuel pyrolysis. Furthermore, the HyChem model is expected to capture the effect of vitiation well because 1) fuel pyrolysis model considers the fuel attack via H-abstraction by both OH and H radicals, and 2) the OH concentration under the vitiated condition is largely governed by the $CH_3 + H_2O$ reaction with a well-studied rate constant. The fact that the methane yield in the vitiated pyrolysis is much larger than the vitiated oxidation (Fig. 4) is because of the higher OH concentration in the vitiated oxidation, which promotes the back reaction of $CH_3+H_2O \rightarrow CH_4+OH$.

In terms of the effect of vitiation, the reaction of JP-10 shares many similarities with that of Jet A, except that the production

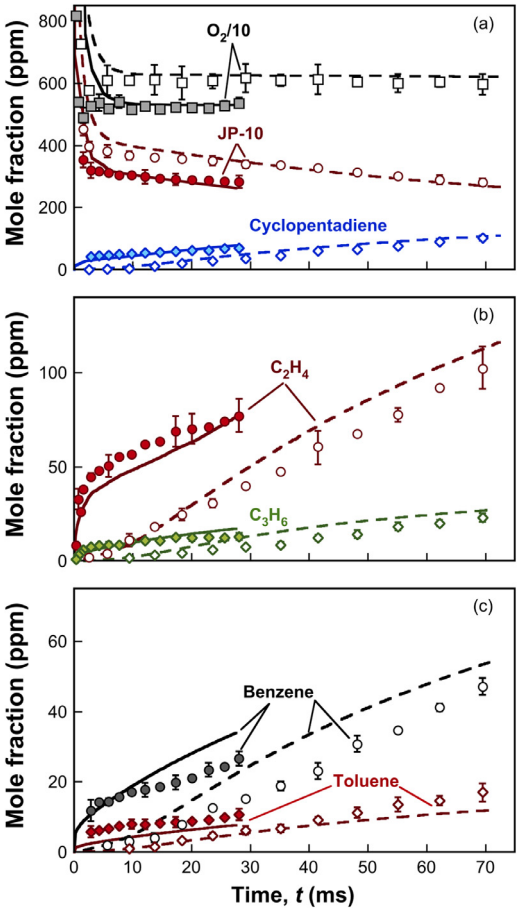

Fig. 5. Experimental (symbols) and computed (lines) species profiles in vitiated and non-vitiated oxidation of JP-10 at 1030 K and 1 atm with $\phi \cong 0.95$. Experiment 5 (vitiated oxidation): filled symbols and solid lines; Experiment 4 (non-vitiated oxidation): open symbols and dashed lines. See Table 1 for experimental conditions. The vertical bars represent scatter in the experimental data from multiple experiments. The computed initial fuel and oxygen mole fraction values are higher than the nominal values given in Table 1 because of the mixing model used in the simulations.

of methane is absent under both vitiated and non-vitiated conditions. Figure 5 shows a comparison of the species profiles for JP-10 oxidation for a non-vitiated experiment (Experiment 4) with a vitiated experiment under similar conditions (Experiment 5). It can be seen that similar to Jet A, vitiation produces a significant reduction in reaction time for a similar fuel conversion. Figure 6 shows the carbon distribution experimentally observed for JP-10 at a fuel conversion (20%) for both vitiated and non-vitiated conditions. The smaller fuel conversion value, as opposed to 47% for Jet A, is chosen here because of the smaller extents of fuel conversion in the JP-10 experiment than the Jet A experiment at the same temperature. The primary effect of vitiation is to increase the reaction rates, but the product yield distribution is largely unaffected by vitiation under the experimental conditions considered. Like Jet A, the insensitivity of the product yield distribution to vitiation extends over a quite wide range of fuel conversion.

Similar to Jet A, the oxidative pyrolysis of JP-10 appears to be decoupled from the oxidation of the resulting pyrolysis products. Unlike Jet A, one of the dominant pyrolysis products of JP-10 is cyclopentadiene (C_5H_6) in addition to ethylene. The HyChem model captures the concentrations of these major species well, but some discrepancies exist for the minor pyrolysis species, including propene and benzene, as seen in Fig. 5. These discrepancies certainly deserve further study. The model reproduces most of the

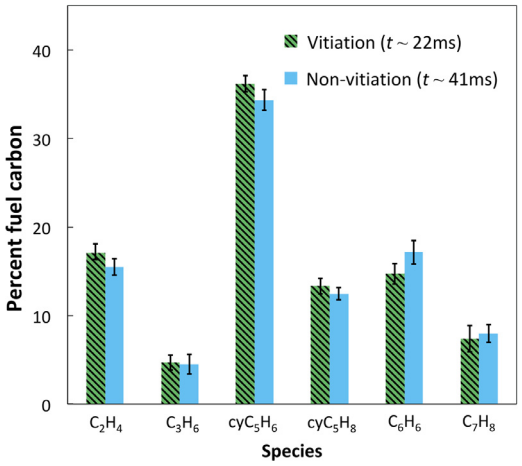

Fig. 6. Experimentally-observed carbon distributions for JP-10 oxidation at ~20% fuel conversion under vitiated and non-vitiated conditions. The vertical bars represent scatter in the experimental data from multiple experiments.

effects of vitiation. Because of the unique decomposition pathway of JP-10, methyl radicals, and hence methane, are not produced in an appreciable quantity. Reaction path analysis reveals that the increase in the overall vitiated oxidative pyrolysis rates are due to OH production. Differently from Jet A, OH is produced from a range of reactions, among which H_2O reacting with H atom provides the highest overall OH production rate:

$$H+H_2O \rightarrow H_2+OH$$

Indeed, H_2 was found to be the most dominant product from vitiated oxidative pyrolysis of JP-10 at a somewhat higher temperature (1130 K) [12]. In addition, analysis shows that $CH_3 + H_2O \rightarrow CH_4 + OH$ also contributes to OH production in vitiated JP-10 oxidative pyrolysis but at an extent much less significant than Jet A.

To address the question raised earlier about the role of vitiation on HyChem model development, we note that four of the stoichiometric parameters were derived from data obtained from the Stanford flow reactor under the vitiated condition for Jet A. These parameters are λ_3 (the C_3H_6-to-C_2H_4 ratio), $\lambda_{4,1}$ (the 1-C_4H_8-to-C_2H_4 ratio), $\lambda_{4,i}$ (the i-C_4H_8-to-C_2H_4 ratio), and χ (the ratio of benzene to the sum of benzene and toluene). For the same Jet A studied here, these ratios are found to be insensitive to vitiation, and under both vitiated and non-vitiated conditions they remain constant over the range of fuel conversions measured (up to 60% for the current experiments as shown in Fig. 3). The lack of sensitivity of these parameters to vitiation explains why the HyChem models reproduce the current non-vitiated experiments satisfactorily, even though the models were developed from a combination of flow reactor experiments under vitiated conditions and shock tube experiments under non-vitiated conditions.

5. Conclusions

In the present study, experiments and modeling were carried out to provide a fundamental understanding of the impact of vitiation on reactivity and product distribution of two different jet fuels in the fuel decomposition region. The primary effect of vitiation is the significant increase in the reactivity of the fuels, but with only a minor impact on the reaction pathways, leading to carbon product distributions for each fuel that were nearly identical under vitiated and non-vitiated conditions. In addition, the presence of oxygen has little impact on yields of pyrolysis products, and there is very little oxygen depletion during fuel breakdown. Vitiation increases the fuel oxidative pyrolysis rate because of the conversion of water into the OH radical, which increases the rate of fuel attack through the H-atom abstraction reaction. The HyChem models for the two fuels adequately captured the effect of vitiation on species profiles in the fuel decomposition region.

Declaration of Competing Interest

The authors declare that they have no known competing financial interests or personal relationships that could have appeared to influence the work reported in this paper.

Acknowledgments

This work was supported by the U.S. Air Force Office of Scientific Research under grant number FA9550-16-1-0195, Dr. Chiping Li, Program Officer.

Supplementary materials

Supplementary material associated with this article can be found, in the online version, at doi:10.1016/j.combustflame.2020.10.044.

References

[1] F.L. Dryer, F.M. Haas, J. Santner, T.I. Farouk, M. Chaos, Interpreting chemical kinetics from complex reaction–advection–diffusion systems: modeling of flow reactors and related experiments, Prog. Energy Combust. Sci. 44 (2014) 19–39.
[2] U. Shrestha, M. Rahimi, G. Simms, H. Chelliah, Fuel pyrolysis in a microflow tube reactor – measurement and modeling uncertainties of ethane, *n*-butane, and *n*-dodecane pyrolysis, Combust. Flame 177 (2017) 10–23.
[3] P.G. Kristensen, P. Glarborg, K. Dam-Johansen, Nitrogen chemistry during burnout in fuel-staged combustion, Combust. Flame 107 (1996) 211–222.
[4] S. Wang, D.L. Miller, N.P. Cernansky, H.J. Curran, W.J. Pitz, C.K. Westbrook, A flow reactor study of neopentane oxidation at 8 atmospheres: experiments and modeling, Combust. Flame 118 (1999) 415–430.
[5] S. Banerjee, R. Tangko, D.A. Sheen, H. Wang, C.T. Bowman, An experimental and kinetic modeling study of *n*-dodecane pyrolysis and oxidation, Combust. Flame 163 (2016) 12–30.
[6] J. Urzay, Supersonic combustion in air-breathing propulsion systems for hypersonic flight, Ann. Rev. Fluid Mech. 50 (2018) 593–627.
[7] C. Xu, A.Y. Poludnenko, X. Zhao, H. Wang, T. Lu, Structure of strongly turbulent premixed *n*-dodecane–air flames: direct numerical simulations and chemical explosive mode analysis, Combust. Flame 209 (2019) 27–40.
[8] M. Chan, S. Das, R.D. Reitz, Modeling multiple injection and EGR effects on diesel engine emissions, SAE Trans. 106 (1997) 1072–1093.
[9] J.A. Wünning, J.G. Wünning, Flameless oxidation to reduce thermal NO-formation, Prog. Energy Combust. Sci. 23 (1997) 81–94.
[10] H. Wang, R. Xu, K. Wang, C.T. Bowman, R.K. Hanson, D.F. Davidson, K. Brezinsky, F.N. Egolfopoulos, A physics-based approach to modeling real-fuel combustion chemistry – I. Evidence from experiments, and thermodynamic, chemical kinetic and statistical considerations, Combust. Flame 193 (2018) 502–519.
[11] R. Xu, K. Wang, S. Banerjee, J. Shao, T. Parise, Y. Zhu, S. Wang, A. Movaghar, D.J. Lee, R. Zhao, X. Han, Y. Gao, T. Lu, K. Brezinsky, F.N. Egolfopoulos, D.F. Davidson, R.K. Hanson, C.T. Bowman, H. Wang, A physics-based approach to modeling real-fuel combustion chemistry – II. Reaction kinetic models of jet and rocket fuels, Combust. Flame 193 (2018) 520–537.
[12] Y. Tao, R. Xu, K. Wang, J. Shao, S.E. Johnson, A. Movaghar, X. Han, J.-W. Park, T. Lu, K. Brezinsky, F.N. Egolfopoulos, D.F. Davidson, R.K. Hanson, C.T. Bowman, H. Wang, A physics-based approach to modeling real-fuel combustion chemistry – III. Reaction kinetic model of JP10, Combust. Flame 198 (2018) 466–476.
[13] K. Wang, C.T. Bowman, H. Wang, Kinetic analysis of distinct product generation in oxidative pyrolysis of four octane isomers, Proc. Combust. Inst. 37 (2019) 531–538.
[14] C. Schmidt, C.T. Bowman, Flow reactor study of the effect of pressure on the thermal de-NO_x process, Combust. Flame 127 (2001) 1958–1970.
[15] K. Walters, C.T. Bowman, Vitiated ethane oxidation in a high-pressure flow reactor, Combust. Flame 156 (2009) 1886–1897.
[16] K. Wang, R. Xu, T. Parise, J. Shao, A. Movaghar, D.J. Lee, J.-W. Park, Y. Gao, T. Lu, F.N. Egolfopoulos, D.F. Davidson, R.K. Hanson, C.T. Bowman, H. Wang, A physics-based approach to modeling real-fuel combustion chemistry – IV. HyChem modeling of combustion kinetics of a bio-derived jet fuel and its blends with a conventional Jet A, Combust. Flame 198 (2018) 477–489.
[17] M. Colket, J. Heyne, M. Rumizen, M. Gupta, T. Edwards, W.M. Roquemore, G. Andac, R. Boehm, J. Lovett, R. Williams, Overview of the national jet fuels combustion program, AIAA J. 55 (2017) 1087–1104.
[18] T.N. Zwietering, A backmixing model describing micromixing in single-phase continuous-flow systems, Chem. Eng. Sci 39 (1984) 1765–1778.

[19] T. Malewicki, K. Brezinsky, Experimental and modeling study on the pyrolysis and oxidation of *n*-decane and *n*-dodecane, Proc. Combust. Inst. 34 (2013) 361–368.
[20] D. Davidson, Z. Hong, G. Pilla, A. Farooq, R. Cook, R. Hanson, Multi-species time-history measurements during *n*-heptane oxidation behind reflected shock waves, Combust. Flame 157 (2010) 1899–1905.
[21] D. Davidson, Z. Hong, G. Pilla, A. Farooq, R. Cook, R. Hanson, Multi-species time-history measurements during *n*-dodecane oxidation behind reflected shock waves, Proc. Combust. Inst. 33 (2011) 151–157.
[22] R. Xu, H. Wang, A physics-based approach to modeling real-fuel combustion chemistry – VII. Relationship between speciation measurement and reaction model accuracy, Combust. Flame (2020), doi:10.1016/j.combustflame.2020.10.023.